

Anisotropic superconducting properties of Kagome metal CsV_3Sb_5

Shunli Ni(倪顺利)^{1,2†}, Sheng Ma (马晟)^{1,2†}, Yuhang Zhang(张宇航)^{1,2†}, Jie Yuan(袁洁)^{1,2,5}, Haitao Yang(杨海涛)^{1,2,3,5*}, Zouyouwei Lu(鲁邹有为)^{1,2}, Ningning Wang(王宁宁)^{1,2}, Jianping Sun(孙建平)^{1,2}, Zhen Zhao(赵振)^{1,2}, Dong Li(李栋)^{1,2}, Shaobo Liu(刘少博)^{1,2}, Hua Zhang(张华)^{1,2}, Hui Chen(陈辉)^{1,2,3,5}, Kui Jin(金魁)^{1,2,5}, Jinguang Cheng(程金光)^{1,2}, Li Yu(俞理)^{1,2,5*}, Fang Zhou(周放)^{1,2,5}, Xiaoli Dong(董晓莉)^{1,2,5*}, Jiangping Hu(胡江平)^{1,4}, Hong-Jun Gao(高鸿钧)^{1,2,3,5}, and Zhongxian Zhao(赵忠贤)^{1,2,5}

¹ *Beijing National Laboratory for Condensed Matter Physics and Institute of Physics,
Chinese Academy of Sciences, Beijing 100190, China*

² *University of Chinese Academy of Sciences, Beijing 100049, China*

³ *CAS Center for Excellence in Topological Quantum Computation, University of Chinese
Academy of Sciences, Beijing 100190, PR China*

⁴ *Kavli Institute of Theoretical Sciences, University of Chinese Academy of Sciences, Beijing,
100190, China*

⁵ *Songshan Lake Materials Laboratory, Dongguan, Guangdong 523808, China*

[†]These authors contributed equally to this work

*E-mail: li.yu@iphy.ac.cn (L.Y.); htyang@iphy.ac.cn (H.Y.); dong@iphy.ac.cn (X.D.)

Abstract

We measure the superconducting properties of high-quality CsV_3Sb_5 single crystals with $T_c \sim 3.5$ K. We find that the upper critical field $H_{c2}(T)$ exhibits a large anisotropic ratio H_{c2}^{ab}/H_{c2}^c up to 9 at zero temperature and fitting its temperature dependence requires a minimum two-band effective model. The ratio of the lower critical field H_{c1}^{ab}/H_{c1}^c is also found to be larger than 1, which indicates that the in-plane energy dispersion is strongly renormalized near Fermi energy. Furthermore, we find a two-fold anisotropy in the in-plane angular-dependent magnetoresistance in the mixed state. Interestingly, below a characteristic temperature of 2.8 K, the orientation of this anisotropy displays a peculiar twist by an angle of 60° characteristic of the Kagome geometry. The results suggest an intriguing superconducting state with coexisted intertwined orders, which, at least, are partially driven by electron-electron correlation.

Quasi-two-dimensional (2D) transition metal Kagome system serves as an important playground to study various electronic phenomena in the presence of geometric frustration and nontrivial band topology ^[1-12]. It can host frustrated magnetism, anomalous Hall effect, and various charge orders. The recently discovered AV_3Sb_5 ($A = K, Rb, Cs$) is a new class of Kagome family with bulk superconductivity at $T_c \sim 2.5$ K ^[13-15]. Some experimental results suggest unconventional pairing nature in such Kagome system ^[13,16-19]. In addition, an exotic charge density wave (CDW)-like order can be identified at $T^* \sim 78 - 104$ K in the normal state ^[11,13-15,18,20-26], and coexists with the superconductivity at lower temperatures. The chirality of such charge order is further verified by scanning tunneling microscopy (STM) measurements ^[18,20,24,26], which can partially explain the giant anomalous Hall effect (AHE) in the system ^[23,27]. Recent transport measurements under pressure reveal that superconducting dome appears as the charge order is suppressed by pressure ^[17,21,22,28,29]. All these findings suggest the rich and novel physics behind the superconductivity in the AV_3Sb_5 system. However, a systematic characterization of the fundamental superconducting parameters, like lower (upper) critical fields H_{c1} (H_{c2}), magnetic penetration depth λ , coherence length ξ , is still lacking.

Here we present systematic magnetic and electrical transport measurements of high-quality single crystals of CsV_3Sb_5 showing a higher $T_c \sim 3.5$ K. The upper critical field exhibits a large anisotropic ratio H_{c2}^{ab}/H_{c2}^c up to 9 at zero temperature, and the fitting to the $H_{c2}(T)$ data requires a minimum two-band effective model. These are consistent with the quasi-2D and multiband nature ^[23,27] reported previously. Nevertheless, the lower critical field along *ab*-plane (H_{c1}^{ab}) is found to be higher than that along *c*-axis (H_{c1}^c). The in-plane and out-of-plane superconducting coherence length and penetration depth are also deduced. Furthermore, a two-fold anisotropy in the in-plane angular-dependent magnetoresistance is identified in the mixed state. Intriguingly, below a characteristic temperature of 2.8 K, the orientation of this anisotropy displays a twist by an angle of 60° characteristic of the Kagome lattice. Our findings will shed more light on the understanding of the rich physics embedded in this novel superconducting Kagome system.

The CsV_3Sb_5 single crystals were synthesized by the self-flux method ^[13-15,23,27,29,30]. The x-ray diffraction (XRD) data were collected at room temperature on a diffractometer (Rigaku SmartLab, 9kW) equipped with two Ge (220) monochromators. The magnetic property measurements were conducted on a Quantum Design MPMS-XL1 system down to 1.8 K, and a MPMS-3 system

equipped with an iHe3 insert down to 0.4 K. The electrical transport properties were measured on a Quantum Design PPMS-9 system under fields up to 8 T.

The representative XRD pattern of the CsV_3Sb_5 single crystals, shown in the upper right inset of Fig. 1a, confirms the single preferred (001) orientation. The lattice parameter c is calculated to be 9.318 Å, consistent with previous reports [23,30]. The double-crystal x-ray rocking curve for the (008) Bragg reflection (Fig. 1a) exhibits a small crystal mosaic of 0.24° in terms of the full width at half maximum (FWHM), demonstrating an excellent out-of-plane crystalline perfection. The φ -scan of the (202) plane in Fig. 1b displays six successive peaks with an equal interval of 60°, in accordance with the hexagonal symmetry of the Kagome lattice. The superconductivity of the CsV_3Sb_5 single crystal is confirmed by the superconducting diamagnetism at an onset $T_c \sim 3.5$ K as shown in Fig. 1c, as well as by the zero resistance at ~ 3.0 K as seen in Fig. 1d. We note that the previous work usually reports the superconductivity at a $T_c \sim 2.5 - 2.8$ K [13,17,21,23,24,31] in this Kagome system, which is lower than the T_c and zero-resistance temperature observed here in our sample. However, the superconducting transition is not as sharp as expected for the high-quality sample. It is noticeable that, the diamagnetic signal gently sets in below ~ 3.5 K, as shown in Fig. 1c, then it abruptly drops around ~ 2.8 K, followed by the 100 % superconducting shielding. Such a two-stage-like transition seems common in the CsV_3Sb_5 single crystals studied by different groups [13,17,21,23].

In order to obtain the upper critical field $H_{c2}(T)$ of the sample, the magnetoresistance $R(T, H)$ data were collected under various fields along the c axis and ab plane. As shown in Fig. 2a and 2b, the resistive transitions show no significant broadening in the magnetic fields. The temperature dependences of the obtained in-plane $H_{c2}^{ab}(T)$ and out-of-plane $H_{c2}^c(T)$ show positive curvature. Accordingly, the $H_{c2}(T)$ behavior is well fitted by a two-band model [32] rather than the single-band WHH formula [33] (Fig. 2c), consistent with the multiband nature [23,27]. The zero-temperature $H_{c2}(0)$ is estimated to be 0.8 T for $H//c$ and 7.2 T for $H//ab$. The deduced in-plane coherence length is $\xi_{ab}(0) = 20.3$ nm, and the out-of-plane one $\xi_c(0) = 2.2$ nm. The anisotropy $\gamma = \xi_{ab}/\xi_c \sim 9$, comparable with that of quasi-2D cuprate and iron-based superconductors.

The temperature dependence of lower critical fields H_{c1} can also provide important information of the multiband superconductivity in the Kagome metal CsV_3Sb_5 . The measurements of isothermal magnetization $M(H)$ with magnetic field along the c axis and ab plane are respectively presented in Fig. 3a and b. The

temperature dependences of the obtained H_{c1}^c and H_{c1}^{ab} are plotted in Fig. 3c and d, respectively. Unusual behavior of the lower critical fields is evident. As the system enters the superconducting state, both H_{c1}^c and H_{c1}^{ab} are nearly temperature-independent, corresponding to the gentle increase of diamagnetism with temperature. Below a characteristic temperature $T = 2.8$ K, both H_{c1}^c and H_{c1}^{ab} rise abruptly with cooling, coinciding with the significant increase in the Meissner and shielding signal sizes. The temperature dependences of H_{c1}^c and H_{c1}^{ab} are fitted by a semi-classical approach ^[34] with different models, including single band *s*-wave, *d*-wave and a simple two-gap one, as shown in Fig. 3c and 3d. Obviously, the two-gap model gives the best fit for H_{c1}^c , yielding a London penetration depth $\lambda_{ab}(0) \sim 460$ nm in agreement with that estimated by tunneling diode oscillator ^[19].

It is noteworthy that, the value of lower critical field H_{c1}^{ab} is found to be higher than that of H_{c1}^c , while the H_{c2} exhibits a much larger anisotropic ratio of $H_{c2}^{ab}(0)/H_{c2}^c(0)$ as mentioned above. The results of H_{c1} suggest that the effective in-plane electron mass (m_{ab}) is larger than the out-of-plane effective mass (m_c), which is inconsistent with the large anisotropy revealed by H_{c2} data. However, as suggested in theory ^[11,12], the electronic physics in this material is likely driven by the Kagome Van Hove points. In this case, the effect of the electron-electron correlation becomes important and the band dispersion near Fermi energy can be strongly renormalized. Thus, combining the presence of Van Hove physics and electron-electron correlation, the in-plane effective mass can be strongly enhanced.

To further investigate the unusual electronic and superconducting properties of CsV_3Sb_5 system, the in-plane angular-dependent magnetoresistance (AMR) are measured under a field of 0.5 T at different temperatures in the mixed state. As shown in Fig. 4a, AMR exhibits a pronounced *two-fold* rotational symmetry, and, to our knowledge, such anisotropy in this system has never been reported before. To estimate the strength of relative change of the anisotropic AMR signal, the ratio $\Delta R/R_{\min} = (R(\theta,T) - R_{\min}(T))/R_{\min}(T) \times 100\%$ is summarized in the polar-coordinate plots in Fig. 4b. A large change of $\sim 50\%$ in AMR is observed, despite the quick reduction of the absolute values with lowering temperature, as shown in Fig. 4a. This reflects the field-induced anisotropic dissipation part in the mixed state of CsV_3Sb_5 system.

We note that significant two-fold anisotropy of in-plane AMR has also been observed in the topological superconductor of trigonal $\text{Sr}_{0.10}\text{Bi}_2\text{Se}_3$ under a 0.4 T field in the mixed state ^[35]. In that case, however, the line-shape of $R(\theta)$ changes

significantly with temperature, which is distinct from our observation in CsV_3Sb_5 (Fig. 4a). Furthermore, it is intriguing that, as the present hexagonal CsV_3Sb_5 is cooled below the characteristic temperature of 2.8 K, the maximum direction of the anisotropic AMR rotates by an angle of 60° with respect to the original one, shown in Fig. 4a and b. Such a peculiar twist of AMR orientation seems to coincide with the Kagome symmetry and its origin is not yet clear. Nevertheless, this mysterious rotation must relate to the electronic and crystallographic environments, which host variable flux dissipation intertwined with certain coexisting orders in the superconducting mixed state. The AMR anisotropy induced by mild in-plane field and its temperature sensitivity observed here imply a contribution from the spin degree of freedom and a weak coupling to the crystal lattice. Further investigation is certainly required for a better understanding of the physics behind such exotic rotation.

In summary, we have carried out systematic magnetic and electrical transport measurements of high-quality single crystals of CsV_3Sb_5 showing a higher $T_c \sim 3.5$ K. Our experimental results are consistent with a quasi-2D multiband superconductor. The lower critical field also suggests a strongly renormalized in-plane effective mass, which indicates the presence of correlated electronic physics due to Van Hove points near Fermi energy. Our finding of a two-fold anisotropy in the in-plane angular-dependent magnetoresistance and its twist by an angle of 60° suggests rich physics due to the coexistence of intertwined orders in the superconducting state. Our findings will shed new light on the understanding of the rich physics embedded in this novel superconducting Kagome system.

Acknowledgement

This work is supported by the National Science Foundation of China (Grant Nos. 11834016, 11888101, 12061131005, 51771224, and 61888102), the National Key Research and Development Projects of China (Grant Nos. 2017YFA0303003 and 2018YFA0305800), the Key Research Program and Strategic Priority Research Program of Frontier Sciences of the Chinese Academy of Sciences (Grant Nos. QYZDY-SSW-SLH001, XDB33010200, and XDB25000000).

Reference

- [1] Anderson P W 1973 *Mater. Res. Bull.* **8**, 153
- [2] Ran Y, Hermele M, Lee P A, and Wen X-G 2007 *Phys. Rev. Lett.* **98**, 117205
- [3] Balents L 2010 *Nature* **464**, 199
- [4] Lin Z, Choi J-H, Zhang Q, Qin W, Yi S, Wang P, Li L, Wang Y, Zhang H, Sun Z, Wei L, Zhang S, Guo T, Lu Q, Cho J-H, Zeng C, and Zhang Z 2018 *Phys. Rev. Lett.* **121**, 096401
- [5] Yin J-X, Zhang S S, Chang G, Wang Q, Tsirkin S S, Guguchia Z, Lian B, Zhou H, Jiang K, Belopolski I, Shumiya N, Multer D, Litskevich M, Cochran T A, Lin H, Wang Z, Neupert T, Jia S, Lei H, and Hasan M Z 2019 *Nat. Phys.* **15**, 443
- [6] Ye L, Kang M, Liu J, Von Cube F, Wicker C R, Suzuki T, Jozwiak C, Bostwick A, Rotenberg E, Bell D C, Fu L, Comin R, and Checkelsky J G 2018 *Nature* **555**, 638
- [7] Yin J-X, Zhang S S, Li H, Jiang K, Chang G, Zhang B, Lian B, Xiang C, Belopolski I, Zheng H, Cochran T A, Xu S-Y, Bian G, Liu K, Chang T-R, Lin H, Lu Z-Y, Wang Z, Jia S, Wang W, and Hasan M Z 2018 *Nature* **562**, 91
- [8] Liu E, Sun Y, Kumar N, Muechler L, Sun A, Jiao L, Yang S-Y, Liu D, Liang A, Xu Q, Kroder J, Süß V, Borrmann H, Shekhar C, Wang Z, Xi C, Wang W, Schnelle W, Wirth S, Chen Y, Goennenwein S T B, and Felser C 2018 *Nat. Phys.* **14**, 1125
- [9] Kang M, Ye L, Fang S, You J-S, Levitan A, Han M, Facio J I, Jozwiak C, Bostwick A, Rotenberg E, Chan M K, McDonald R D, Graf D, Kaznatcheev K, Vescovo E, Bell D C, Kaxiras E, Van Den Brink J, Richter M, Prasad Ghimire M, Checkelsky J G, and Comin R 2020 *Nat. Mater.* **19**, 163
- [10] Eric M K, Brenden R O, Chennan W, Stephen D W, and Michael G 2021 *J. Phys.-Condens. Matt.*, accepted
- [11] Tan H, Liu Y, Wang Z, and Yan B 2021, arXiv:2103.06325 [cond-mat.supr-con]
- [12] Feng X, Jiang K, Wang Z, and Hu J 2021, arXiv:2103.07097 [cond-mat.supr-con]
- [13] Ortiz B R, Teicher S M L, Hu Y, Zuo J L, Sarte P M, Schueller E C, Abeykoon A M M, Krogstad M J, Rosenkranz S, Osborn R, Seshadri R, Balents L, He J, and Wilson S D 2020 *Phys. Rev. Lett.* **125**, 247002
- [14] Ortiz B R, Sarte P M, Kenney E M, Graf M J, Teicher S M L, Seshadri R, and Wilson S D 2021 *Phys. Rev. Mater.* **5**, 034801
- [15] Qiangwei Yin Z T, Chunsheng Gong, Yang Fu, Shaohua Yan, and Lei H 2021 *Chin. Phys. Lett.* **3**, 037403
- [16] Wang Y, Yang S, Sivakumar P K, Ortiz B R, Teicher S M L, Wu H, Srivastava A K, Garg C, Liu D, Parkin S S P, Toberer E S, McQueen T, Wilson S D, and Ali M N 2020, arXiv:2012.05898

[cond-mat.supr-con]

- [17] Zhao C C, Wang L S, Xia W, Yin Q W, Ni J M, Huang Y Y, Tu C P, Tao Z C, Tu Z J, Gong C S, Lei H C, Guo Y F, Yang X F, and Li S Y 2021, arXiv:2102.08356 [cond-mat.supr-con]
- [18] Chen H, Yang H, Hu B, Zhao Z, Yuan J, Xing Y, Qian G, Huang Z, Li G, Ye Y, Yin Q, Gong C, Tu Z, Lei H, Ma S, Zhang H, Ni S, Tan H, Shen C, Dong X, Yan B, Wang Z, and Gao H-J 2021, arXiv:2103.09188 [cond-mat.supr-con]
- [19] Duan W, Nie Z, Luo S, Yu F, Ortiz B R, Yin L, Su H, Du F, Wang A, Chen Y, Lu X, Ying J, Wilson S D, Chen X, Song Y, and Yuan H 2021, arXiv:2103.11796 [cond-mat.supr-con]
- [20] Jiang Y-X, Yin J-X, Denner M M, Shumiya N, Ortiz B R, He J, Liu X, Zhang S S, Chang G, Belopolski I, Zhang Q, Shafayat Hossain M, Cochran T A, Multer D, Litskevich M, Cheng Z-J, Yang X P, Guguchia Z, Xu G, Wang Z, Neupert T, Wilson S D, and Zahid Hasan M 2020, arXiv:2012.15709 [cond-mat.supr-con]
- [21] Chen K Y, Wang N N, Yin Q W, Tu Z J, Gong C S, Sun J P, Lei H C, Uwatoko Y, and Cheng J-G 2021, arXiv:2102.09328 [cond-mat.supr-con]
- [22] Du F, Luo S, Ortiz B R, Chen Y, Duan W, Zhang D, Lu X, Wilson S D, Song Y, and Yuan H 2021, arXiv:2102.10959 [cond-mat.supr-con]
- [23] Yu F H, Wu T, Wang Z Y, Lei B, Zhuo W Z, Ying J J, and Chen X H 2021, arXiv:2102.10987 [cond-mat.supr-con]
- [24] Liang Z, Hou X, Ma W, Zhang F, Wu P, Zhang Z, Yu F, Ying J-J, Jiang K, Shan L, Wang Z, and Chen X-H 2021, arXiv:2103.04760 [cond-mat.supr-con]
- [25] Uykur E, Ortiz B R, Wilson S D, Dressel M, and Tsirlin A A 2021, arXiv:2103.07912 [cond-mat.str-el]
- [26] Li H X, Zhang T T, Pai Y-Y, Marvinney C, Said A, Yilmaz T, Yin Q, Gong C, Tu Z, Vescovo E, Moore R G, Murakami S, Lei H C, Lee H N, Lawrie B, and Miao H 2021, arXiv:2103.09769 [cond-mat.supr-con]
- [27] Yang S-Y, Wang Y, Ortiz B R, Liu D, Gayles J, Derunova E, Gonzalez-Hernandez R, Smejkal L, Chen Y, Parkin S S P, Wilson S D, Toberer E S, Mcqueen T, and Ali M N 2020 *Sci. Adv.* **6**, eabb6003
- [28] Zhang Z, Chen Z, Zhou Y, Yuan Y, Wang S, Zhang L, Zhu X, Zhou Y, Chen X, Zhou J, and Yang Z 2021, arXiv:2103.12507 [cond-mat.supr-con]
- [29] Chen X, Zhan X, Wang X, Deng J, Liu X-B, Chen X, Guo J-G, and Chen X 2021, arXiv:2103.13759 [cond-mat.supr-con]
- [30] Ortiz B R, Gomes L C, Morey J R, Winiarski M, Bordelon M, Mangum J S, Oswald L W H, Rodriguez-Rivera J A, Neilson J R, Wilson S D, Ertekin E, Mcqueen T M, and Toberer E S 2019 *Phys. Rev. Mater.* **3**, 094407
- [31] Zhao H, Li H, Ortiz B R, Teicher S M L, Park T, Ye M, Wang Z, Balents L, Wilson S D, and Zeljkovic I 2021, arXiv:2103.03118 [cond-mat.supr-con]
- [32] Gurevich A 2003 *Phys. Rev. B* **67**, 184515
- [33] Werthamer N R, Helfand E, and Hohenberg P C 1966 *Phys. Rev.* **147**, 295
- [34] Prozorov R and Giannetta R W 2006 *Supercond. Sci. Technol.* **19**, R41
- [35] Pan Y, Nikitin A M, Araizi G K, Huang Y K, Matsushita Y, Naka T, and De Visser A 2016 *Sci. Rep.* **6**, 7, 28632

Figure 1

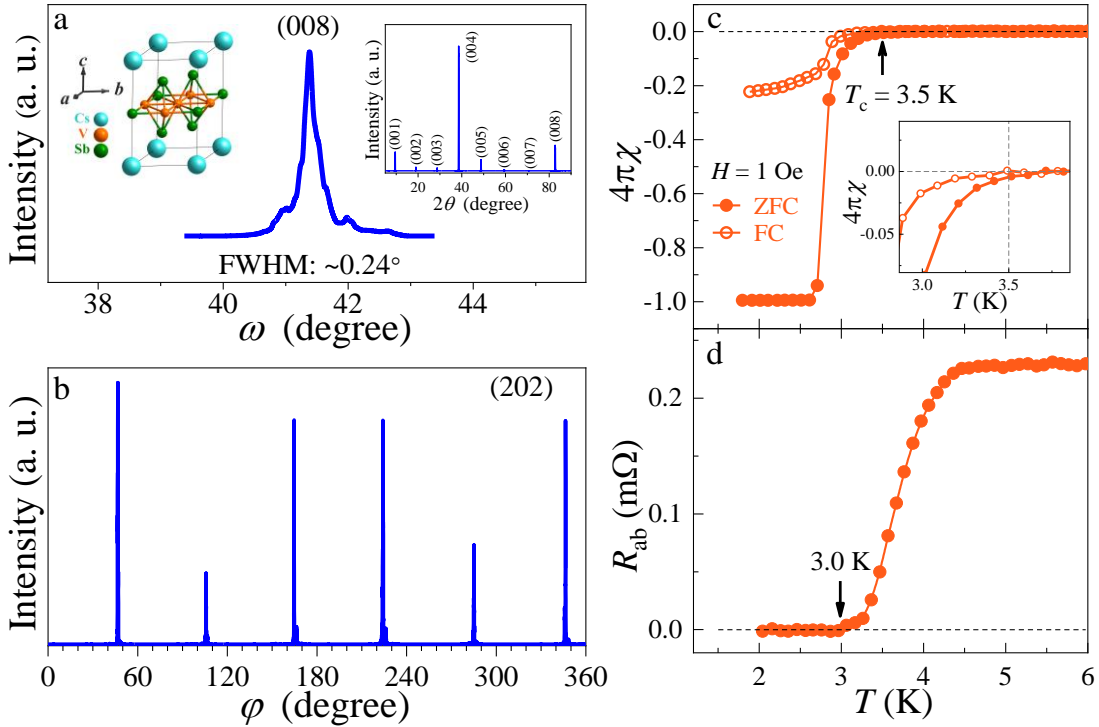


Fig. 1. XRD and superconductivity characterizations of CsV_3Sb_5 single crystal. (a) The rocking curve of (008) reflection with a small FWHM of 0.24° . The left and right insets display the crystal structure and x-ray $\theta - 2\theta$ scan, respectively. (b) The x-ray φ -scan of the (202) plane. (c) The magnetic susceptibilities under zero-field cooling (ZFC) and field cooling (FC), corrected for demagnetization factor. The inset shows the zoom-in superconducting diamagnetism below ~ 3.5 K. (d) Temperature dependence of in-plane resistance shows the zero resistance below ~ 3.0 K.

Figure 2

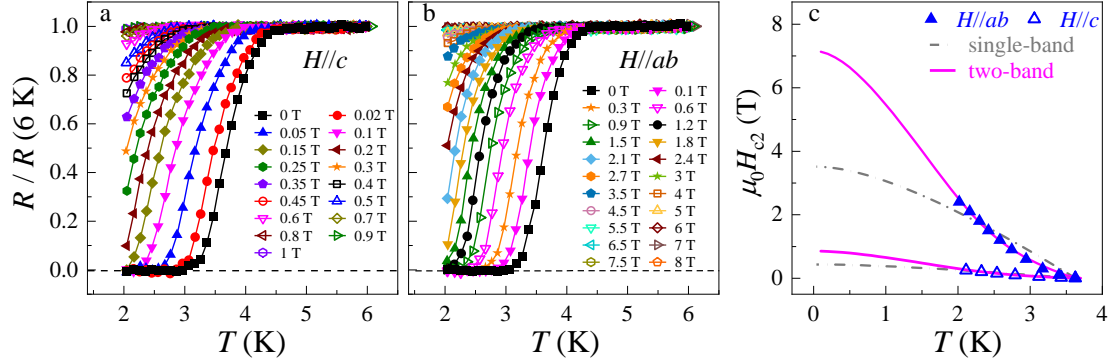


Fig. 2. Normalized in-plane resistance under various magnetic fields up to 8 T and the anisotropic upper critical magnetic fields of the CsV_3Sb_5 single crystal. (a) and (b) are the temperature dependences of normalized in-plane resistance measured under magnetic field along the c axis and ab plane, respectively. (c) Temperature dependences of the anisotropic upper critical fields, obtained from the $R(T)$ data (in (a), (b)) at 50 % of the normal-state resistance. The results of fitting by the two-band (pink solid curve) and single-band WHH (gray point-dashed curve) models are presented.

Figure 3

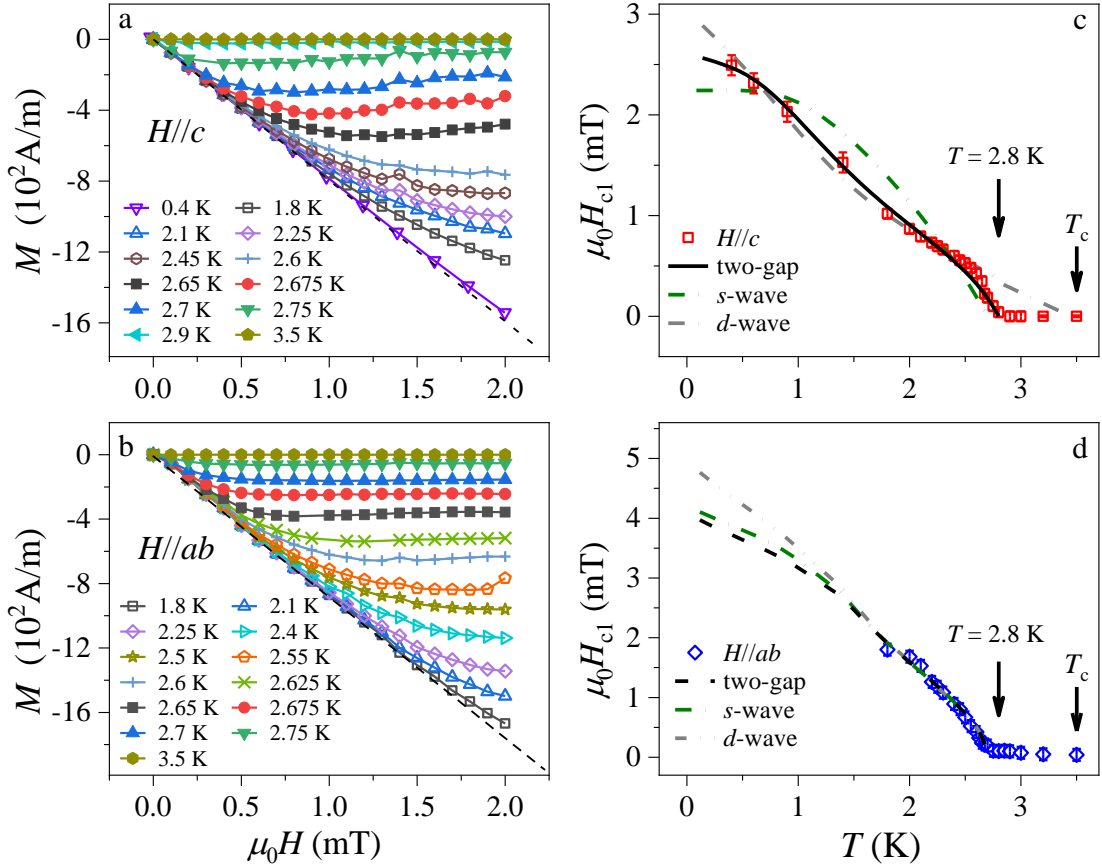


Fig. 3. The measurements of isothermal magnetization and anisotropic low critical magnetic field of the CsV_3Sb_5 single crystal. (a) and (b) show the data of isothermal magnetization, corrected for demagnetization factor, at various temperatures with magnetic field along the c axis and ab plane, respectively. (c) and (d) are the temperature dependences of $\mu_0 H_{c1}$ along the c axis and ab plane, respectively, defined as the fields at which M - H curves start to deviate from the Meissner line ($M/H = -4\pi$, the dashed lines in (a) and (b)). The results of fitting by the two-gap, s -wave and d -wave models are also presented. No difference is detectable among the fittings via the three models for $H \parallel ab$.

Figure 4

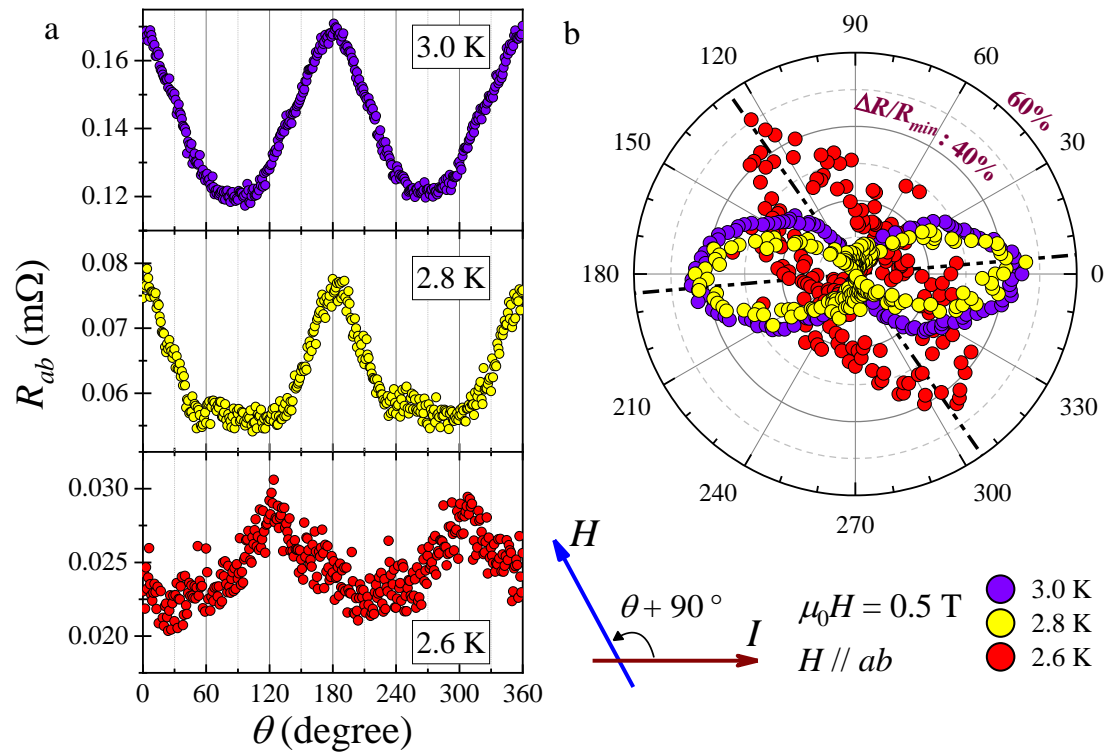


Fig. 4. Temperature dependences of the in-plane angular-dependent magnetoresistance (AMR) in the mixed state. (a) The in-plane AMR as a function of θ . Here θ is the angle between the directions of the external field (H) and the current (I), with $\theta = 0^\circ$ corresponding to $H \perp I$. (b) Polar plots of $\Delta R/R_{\min} = (R(\theta, T) - R_{\min}(T))/R_{\min}(T) \times 100\%$. The two-fold rotational symmetry in AMR is obvious, and the maximum direction of the anisotropic AMR rotates by an angle of 60° below $\sim 2.8 \text{ K}$.